Effects of White Matter on EEG of Multi-layered Spherical Head Models

Md Rezaul Bashar[1,3], Yan Li[1], and Peng Wen[2]

[1]Department of Mathematics and Computing, [2]Faculty of Surveying and Engineering, Centre for Systems Biology, University of Southern Queensland, QLD 4350, Australia
[3]Department of Information and Communication Engineering, Islamic University, Kushtia, Bangladesh
E-mail: {bashar, liyan, pengwen}@usq.edu.au

Abstract - Biological tissues are multi-compartmental inhomogeneous media composed of different cellular and subcellular domains. Human head, a multi-compartmental inhomogeneous medium, is composed of scalp, skull, cerebrospinal fluid (CSF), gray matter (GM), white matter (WM), and other subcellular domains. Among these domains, skull and WM show the complicated anisotropy tissue property because of their physiological structure. However, many researchers model human head excluding WM. This research investigates the necessity of WM using four- and five- layered spherical head models. Four-layered head model excludes WM while five-layered model includes it. The piecewise homogeneous forward model using finite element method is implemented to measure electroencephalogram (EEG) on head surface for both head models. Analyzing these EEGs, this research finds the necessity of using WM to make an accurate human head model.

I. Introduction

Electroencephalogram (EEG) measured from the scalp using electrodes is originated by the neural activity of the brain. This neural activity is modelled with a distribution of current sources. The method of estimating this current distribution is known as EEG source localization or source analysis [1][2][3]. The EEG source analysis is an important tool for diagnosing neurological disorders (such as epilepsy), origin of evoked potentials and in research into cognitive brain functions [1][2]. It is measured by solving the forward and inverse problems [1]. The forward problem is solved by calculating the electrode potentials on scalp for a given source configuration. Inverse problem is solved by iterative solving of forward problem to estimate the current source inside the brain with known electrode potentials [1] [4]. Here is a serious problem that a small error in forward model leads a severe error in inverse model. Therefore, solving forward problem plays a vital rule for accurate source analysis. The solution of forward problem also requires a head or volume conductor model. Volume conductor model ranges from simple homogeneously conducting sphere to complex numerical model consisting millions of elements, each with a different conductivity value [3], for example, the homogeneous sphere model, three-or four-layered concentric model [4], isotropic or anisotropic multi-layered concentric [4], and realistic head models [5]. Zhang *et al.* [6] mentioned that using the homogeneous model to approximate the three-layered concentric model leads to error. Their results recommend that it is better to avoid oversimplified models. The three-layered spherical head model ignores the cerebrospinal fluid (CSF) compartment between the cortex and skull. However, most recently, Wendel *et al.* [7] proved the significant of CSF to construct an accurate head model. In general, these head models assume that the conductivity within a spherical compartment is constant. However, in reality, conductivities at each point in the head are unique, even though they may be of the same tissue type. Moreover, the skull and white matter (WM) of brain compartment exhibit direction related (radial or tangential) conductivities. Previous head construction methods described in different literature neglected WM for anisotropy consideration. However, Hallez *et al.* [8] has shown that neglecting WM anisotropy in the spherical head model arise a 15mm dipole localization error.

Neuronal source localizations based on EEG require a mathematical model in order to compute the electrical potential distribution resulting from dipole or distributed source inside the head. A critical component of source reconstruction is the numerical approximation method used to reach an accurate solution of the associated forward problem. The forward problem requires boundary element method (BEM) or finite element method (FEM) to approximate the solution in addition to source and volume conductor model [5]. In clinical practice, simple volume conductors are still in use, however, recent advances in head modelling techniques make the use of high resolution volume conductor by means of FEM [3]. Only the FEM is able to treat head modelling, electrical properties of each tissue and anisotropy information to include [3][5].

In this paper, we examine how WM affects the scalp potentials to study the effects of WM on constructing an accurate human head model. We generate four-layered spherical head models consisting of scalp, skull, CSF and brain. Again, we generate a five-layered head model consisting gray matter (GM) and WM as separate layer while other layers (scalp, skull and CSF) are identical. We tessellate both head models into approximately the same number of elements. We measure EEG for both head models using FEM with the same electric source. We analyse both EEG models by means of relative difference measure (RDM) and magnification (MAG) error measurements to exhibit the influence of WM.

II. Problem Statement

Conductivity assignment is a critical problem for anisotropic head model generation. To assign proper conductivity to brain tissue, it is to be separated into GM and WM because of their tissue property. To classify brain into GM and WM, we construct two types of head models: i) with the concept of fractional anisotropy (Head model A) and ii) with the concept of effective medium approach (Head model B). In addition, we also mention Head model C to present five-layered model.

A. Head Model A

Li *et al.* [9] classified WM and non-WM tissues from brain tissue layer using fractional anisotropy (FA) based images captured from diffusion tensor magnetic resonance image (DT-MRI) [10]. FA is a technique to measure the extent of the anisotropy property for each voxel (element). Let us suppose that λ_1, λ_2, and λ_3 ($\lambda_1 \geq \lambda_2 \geq \lambda_3$) are the three eigen values of diffusion tensor matrix and λ is the average eigen value. Then FA is defined as [9]:

$$FA = \frac{\sqrt{3}}{\sqrt{2}} \frac{\sqrt{(\lambda_1-\lambda)^2+(\lambda_2-\lambda)^2+(\lambda_3-\lambda)^2}}{\sqrt{\lambda_1^2+\lambda_2^2+\lambda_3^2}} \qquad (1)$$

The FA is in the range from 0 to 1. A fully anisotropic tissue has a factor of FA=1, and an isotropic tissue has a factor FA=0. Kim *et al.* [10] separated WM from non-WM tissues considering WM tissues have larger FA values than non-WM tissues. Applying the FA technique, WM and non-WM tissues are classified according to equation (2) [11]. However, in this research, it is assumed that if FA is less than threshold, the tissue is considered as non-WM; otherwise WM. Non-WM tissues are considered as GM all over this study. Tissue conductivities are randomly selected using the *tissue_type* and isotropic or anisotropic conductivity values are assigned to classified tissues mentioned by the literature [5]. The *tissue_type* is defined as

$$tissue\_type = \begin{cases} 0, & FA < threshold \\ 1, & FA \geq threshold \end{cases} \qquad (2)$$

B. Head model B

In reality, due to the complicated structure and direction of nerve bundles, the anisotropy ratio is not constant every where in the brain [1]. One can estimate diffusion tensor from diffusion weighted MRI (DW-MRI) in each element to determine the direction of nerve bundles. Analysing the diffusion tensor at each element, anisotropic ratio (AR) is defined as the ratio of the largest eigen value to the mean of the two other eigen values [1].

$$AR = \frac{d_1}{mean(d_2, d_3)} \qquad (3)$$

where d_1 is the largest eigen value and d_2, d_3 are two smallest eigen values of the diffusion tensor at a specific element. The values of AR lie between 1 and 10. An element is said to be isotropic where the ratio of d_1 and the mean of d_2 and d_3 are close to 1 ($AR \cong 1$) [1]. Based on this concept, we consider d_1 as longitudinal eigen value as it is the largest eigen value, and d_2 and d_3 are two other transverse eigen values where ($d_1 \geq d_2, d_3$). We also assume the values of these eigen values are determined considering Volume constraint [5], which retains the geometric mean of the eigen values. While we determine *AR*, we apply similar process of Head model A to classify GM and WM as

$$tissue\_type = \begin{cases} 1, & AR < threshold \\ 10, & AR \geq threshold \end{cases} \qquad (4)$$

Classifying the brain tissues, we assign isotropic conductivity to GM and anisotropic conductivity to WM elements and are ready to perform forward computation.

C. Head model C

It is well known that human head is composed of scalp, skull, cerebrospinal fluid (CSF), gray matter (GM), WM, and other sub cellular domains or compartments [6]. Therefore, we construct five-layered spherical head model to represent above mentioned compartments [8][12][13]. Among these compartments, skull and WM show the complicated tissue anisotropy property because of their physiological structure. The anisotropy ratio of WM is considered with the value of 1:10 (transverse: longitudinal) [5][8]. Based on the literature [5][12], the WM conductivity tensor (σ) is assumed and the tensor eigen values are determined considering Volume constraint, as shown in Table 1. Assigning conductivities to each piecewise element, forward computation is performed by means of FEM to measure the electric potentials at scalp.

Table 1 Simulated values for the WM tensor eigen values

σ_{trans}: σ_{long}	σ_{trans}	σ_{long}
1:1 (isotropic)	0.14	0.14
1:2	0.11	0.222
1:4	0.088	0.353
1:8	0.07	0.56
1:10	0.0649	0.65

The electric potentials at scalp are measured by using forward computation with a known current source. The electric field **E** is obtained as the negative gradient of scalar potential, φ, that is $\mathbf{E} = -\nabla\varphi$. According to Ohm's law, the current density **J** and **E** are related as $\mathbf{J} = \sigma\mathbf{E}$, where σ is the conductivity tensor of the medium. In the event that a source density $\mathbf{I}_v$ is present, then $\nabla\mathbf{J} = \mathbf{I}_v$. Finally, the relationship between φ and $\mathbf{I}_v$ can be given as [4][5]

$$\nabla\mathbf{J} = \mathbf{I}_v = -(\nabla \bullet \sigma(\nabla\varphi)) \qquad (5)$$

Equation(5) is solved using Dirichlet and Neumann boundary conditions noting that current can passes only one head layer to another but there is no current getting out of the scalp, respectively [4].

$$\varphi = \varphi_0 \quad \text{on inner surface} \tag{6}$$

$$\sigma(\nabla\varphi) \bullet \mathbf{n} = 0 \quad \text{on outer surface} \tag{7}$$

where $\mathbf{n}$ is unit normal. Some literature found where the analytic solution [8] is used to solve the electric potential problem for isotropic and homogeneous purposes. However, due to complicated head structure, anisotropy and inhomogeneity, some numerical techniques must be employed for solving the forward problem [1][4]. One of the most common numerical techniques is FEM which computes an estimation of the potential field over each element, taking into account the material properties of each individual element. Therefore, it is possible to specify different conductivities over different regions, or even for each element.

We use two error criteria that are commonly used in different literature [4][5][12] to analyse the measured EEGs. We use relative difference measure (RDM) and magnification (MAG) errors, to compare the forward solutions under different conductivity approximations. The minimum RDM value is 0 and MAG value is 1.

III. Implementation and Experimentation

At first, we implement a four-layered spherical head model [4] with different radii for different tissue layers (shown in columns 2 and 3, in Table 2) using Matlab [14] for Head models A and B. Head modelling using FEM requires mesh generation. Mesh represents the piecewise geometry of the head where electric properties are easily included. The first step of mesh generation is to create the surfaces with a given distances d_r from the centre of the spherical head. The second step is the generation of the vertices of the tetrahedral mesh. The third step is the computation of Delaunay triangulation [14] for all generated vertices. The Delaunay triangulation confirms that no vertex resides inside the circumsphere of any generated tetrahedron. In the final step, each generated tetrahedron is labelled as to which each compartment it belongs to. Then the conductivities are assigned to each finite element. We create surfaces with 14 mm thinning for different tissue layers. We mesh the sphere into 315K elements (shown in column 4 in Table 2) from 54K nodes using Tetgen® package provided by Brainstorm [15]. We assign homogeneous isotropic conductivities (shown in last column in Table 2) for different tissue layers according to the literature [4][5] and perform forward computation for the reference model. Later on, we classify the brain layer into GM and WM tissues using Head model A and B techniques implemented in Matlab. Then we assign anisotropic conductivities to WM while isotropic conductivities to GM and other compartments for measurement models. To construct five-layered head model (Head model C), we segment the sphere into five compartments using the same surface thinning of four-layered model. The details of five-layered head model construction are described in our previous papers [12][13]. Brain tissue layers of four-layer model consists 118366 piecewise elements. Analogy, GM consist 66665 elements and 50489 elements are in WM for five-layered model. Approximately, 99% elements of the brain compartment are contained within GM and WM. Moreover, there is a surface between GM and WM. For this model, we segment into approximately the same number of piecewise elements. Table 2 shows the parameters for both head models and Fig. 1 shows the meshed head models. Analogous to previous models, we assign isotropic conductivities to each tissue layer for reference model and we assign WM anisotropic conductivity with the ratio of 1 to 10 (transverse to longitudinal) keeping other compartment isotropic for measurement models. In our research, we consider longitudinal conductivity only.

Table 2 Head model parameters

Head model		Radii	Elements	Isotropic conductivity
Four-layered	scalp	8.8	51792	0.33
	skull	8.5	66427	0.0042
	CSF	8.1	78852	1.00
	brain	7.9	118366	0.33
Five-layered	scalp	8.8	52519	0.33
	skull	8.5	67403	0.0042
	CSF	8.1	78846	1.00
	GM	7.9	66665	0.33
	WM	6.5	50489	0.14

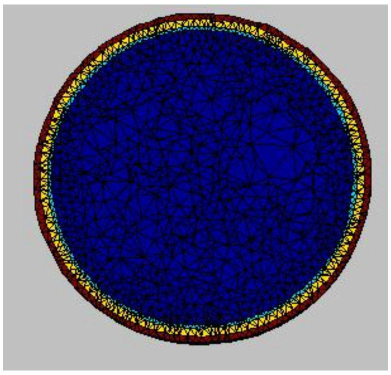

(a)

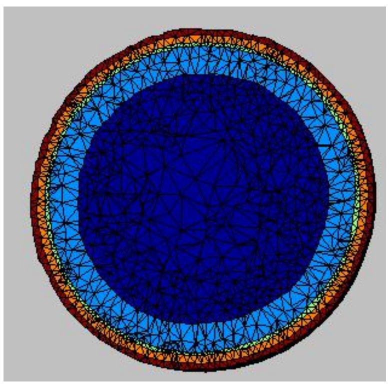

(b)

Fig. 1 Meshed head models: (a) four-layered head model and (b) five-layered head model.

After constructing the head geometry and assigning the conductivities to each layer, we perform the forward computation. As the brain activity can originate from GM only, we assume the dipole located in axial, coronal and sagittal planes. A dipole can be decomposed into three orthogonal dipoles along the main axis, therefore, we consider three orthogonal orientations. These orientations are X orientation (along left-right), Y orientation (along back-front) and Z orientation (along bottom-top). We choose the orientations for the dipole indicated by an azimuth angle $\theta \in [-\pi, \pi]$ and an elevation angel $\varphi \in [-\pi/2, \pi/2]$. We place a fixed dipole at 2mm below the cortex surface inside the GM at the right hemisphere with the value of $\pi/4$ and $\pi/5$ for θ and φ, respectively. We choose the unit magnitude of the dipole. Then we solve equations (5) to (7) using FEM into a set of linear equations. These linear equations are solved by preconditioned conjugate gradient method using Cholesky factorization preconditioning [14] with a drop tolerance of $1e^{-4}$. In this study, 64 electrodes provided by Brainstorm are used to measure the EEG on scalp. Finally, we measure the electric potentials on scalp using the electrodes, where the electrode potentials $\mathbf{V} \in \Re^{m \times 1}$, m is the number of electrodes. We implement these models using an Inter® dual core 2.0 Ghz processor. A single computation for the FEM used in this research takes more than three hours CPU time.

IV. Result Analysis

In this study, we carry out forward computations to measure EEGs for Head models A, B and C independently. For Head model A and B, firstly, we calculate the electric potential differences (EEG) on scalp using the isotropic conductivities for each tissue layer and use for reference model. Then, we logically divide the brain tissue layer into GM and WM based on different thresholds using either Head model A or B. We use 0.2, 0.4, 0.5, 0.6 and 0.9 values for different thresholds. We assign anisotropic conductivities into WM but remaining other tissue layers are isotropic. Finally, we perform forward computation to measure EEGs and we consider these as measurement models.

Fig. 2 shows the RDM and MAG errors generated by Head model A. In this experiment, when we use 0.2 values for threshold, we find very few GM elements (approximately 10% of brain elements). As a result, it generally produces more errors. We also find that the RDM and MAG values are high for 0.2 threshold value. We measure RDM values are between 2.2% and 18%, 17% and 38%, and 3% and 178% for X, Y and Z orientations, respectively. Therefore, on an average, it produces 72% RDM differences. Similarly, it produces 0.58 average MAG errors. When the threshold value is 0.9, RDM and MAG errors exhibit their ideal values because the brain tissue classification based on equation (2) generates 99% GM elements, i.e. as reference model. For other threshold values, the number of elements varies in the resulting variations shown in Fig. 6.

Fig. 3 shows the RDM and MAG errors generated by Head model B. RDM values for X orientation are in the range of 10% to 75%, for Y orientation lie between 8% to 31% and for Z orientation are from 3% to 45% except for the threshold value 9. Therefore, Head model B produces average 43% RDM error. Similarly, it also produces 1.7 average MAG error. For the maximum threshold, it generates the maximum GM elements; as a consequence, it produces the same electrode potentials like the reference model. In this case, we consider 2, 4, 5, 6, and 9 values for AR thresholds defined in equation (4).

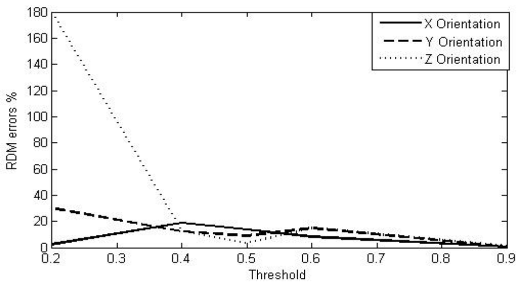

(a)

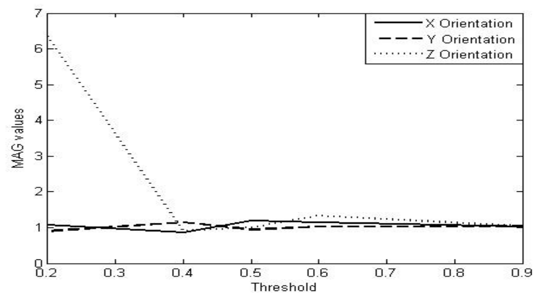

(b)

Fig. 2 RDM and MAG errors produced by reference model and anisotropic model generated by WM anisotropic conductivity using Head model A. (a) presents RDM errors against thresholds and (b) shows MAG values vs thresholds.

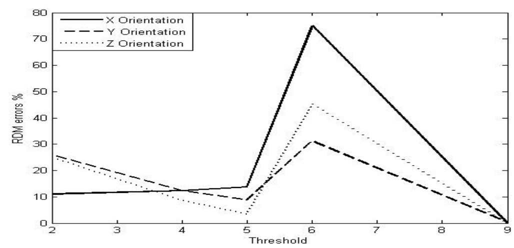

(a)

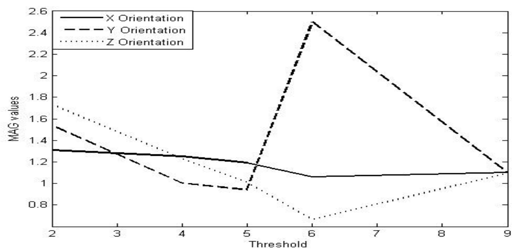

(b)

Fig. 3 RDM and MAG errors produced by reference model and anisotropic model generated by WM anisotropic conductivity using Head model B. (a) presents RDM errors against thresholds and (b) shows MAG values vs thresholds.

Fig. 4 shows the same RDM and MAG errors (shown in Figs. 2 and 3) produced by Head model C with different anisotropy ratios. With the increasing of anisotropy ratio, the conductivity values are also increased, shown in table 1. The more conductivity value increases, the more electrode potential differs from the reference. As the number of WM elements are fixed, it produces smooth upward curves for increasing conductivities with increasing anisotropy ratio. The RDM variation in X orientation is 6%; 4% is for Y orientation and 18% is for Z orientation. Therefore, it produces only 9% average RDM error. It also produces 0.36 average MAG. Analyzing the results produced by Head model A and B shown in Figs. 2 and 3, we observe that Head model C produces less errors than others.

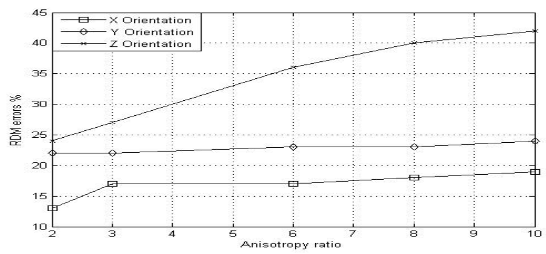

(a)

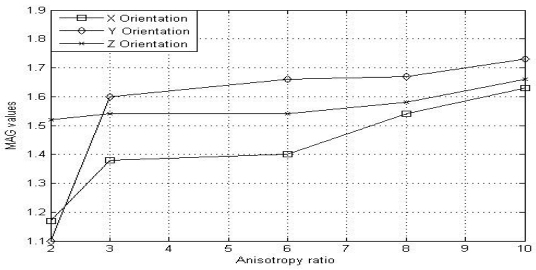

(b)

Fig. 4 RDM and MAG errors for different WM anisotropy ratio on X, Y and Z orientations in Head model C using longitudinal conductivity. (a) Anisotropy ratio vs RDM errors and (b) Anisotropy ratio vs MAG values.

Fig. 5 shows RDM and MAG errors for dipole eccentricity where the more eccentric the dipole, the greater the differences. The dipoles are located at the same places for both four-and five-layered head models. As the depth of GM is limited due to five-layered head model, we place the dipole from 2mm outer the WM surface to 2 mm inner the cortex. As a result, dipole eccentricity starts from 0.8 and finishes to 0.87. For the reference EEG of this computation, we assume the dipole is located at 2mm outer the WM surface. Comparing the errors, we realise that four-layered head model produces more errors than five-layered head models. For instance, the maximum RDM and MAG differences between these two head models for X orientation are 0.6% and 0.0148, respectively, where the eccentricity is 0.87 (the point closer to cortex).

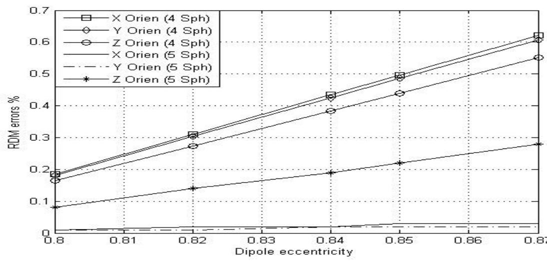

(a)

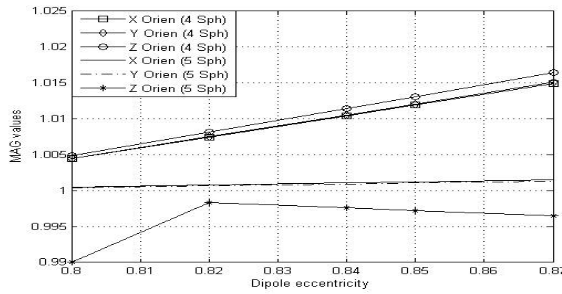

(b)

Fig. 5 Dipole eccentricity for X, Y and Z orientations for four- and five- layered spherical head model. (a) Dipole eccentricity vs RDM errors and (b) Dipole eccentricity vs MAG values.

V. Discussion

In this paper, we have investigated the effects of WM on EEG scalp potentials to analyze the influence of WM to construct an accurate head model for forward as well as inverse computations. Most of the spherical head models are either three- or four-layered. However, there is limited spherical head model consisting five layers. In reality, it is difficult to segment GM and WM from brain. Moreover, the cortex (the outer part of the brain) and thalamus (the core part of the brain) area are belonged to GM. So, there arises a question is it necessary to separate GM and WM from the brain tissue layer?

The classification of brain tissue has an important application in studying the structure and function of the brain [9]. Diffusion coefficient of water molecule in brain tissue decreases quickly after stroke and other brain injuries by thirty to forty percentages [16]. Diffusion tensor imaging (DTI) is widely used in the study and diagnosis of neurological diseases involving in the WM such as stroke, tumors, multiple sclerosis, dyslexia, and schizophrenia [16]. However, many neurological and neurodegenerative diseases, such as Alzheimer's and Creutzfeldt-Jakob diseases are generally considered involving the GM [17]. Thus, it becomes necessary to separate GM and WM to study and investigate neuronal diseases. On the other hand, most head models in different literature assume an isotropic conductivity for brain tissues. However, GM has isotropic and WM has anisotropic conductivities. As spherical head models are easy to construct, many researchers use it to analyze scalp potentials or source reconstruction. Using spherical head models, we have shown that the head model consisting WM produces less average errors than the head model excluding WM. Therefore, we consider that it is important to classify the brain and we suggest that excluding WM compartment will be a cause of inaccurate head model construction, which will greatly affect on the EEG source reconstruction.

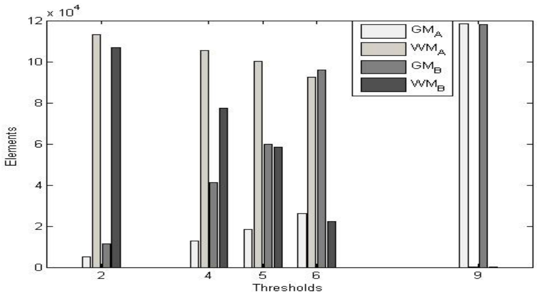

Fig. 6 Number of classified elements for GM and WM of Head model A and Head model B based on different thresholds. In the figure, subscript A represents Head model A and B represents Head model B. Thresholds of Head model A is multiplied by 10.

GM and WM are classified according to either Head model A or B by means of different thresholds, as shown in Fig. 6. Errors are changing with the changing of thresholds (Fig. 2 and Fig. 3). From Fig. 6, when threshold=5, it produces 59663 and 58703 elements for GM and WM, respectively, for Head model B. Coincidentally, we get the close numbers of GM and WM elements to those elements of Head model C. The RDM and MAG errors shown in Fig. 3 are close to those errors produced by Head model C (shown in Fig. 4) for the maximum anisotropy ratio. While for threshold=9, the number of GM elements is 118242, that is most of the brain elements. Therefore, it produces the minimum errors. As no brain signal can be generated from WM, we are bound to locate the dipole inside the GM. In the five-layered head model, the width of GM is 14mm. In reality, the GM is located at the cortex, thalamus and cerebellum region. Therefore, dipoles can be placed at any position within these regions. We shall investigate more similar studies on realistic head model using MRI in the near future.

VI. Conclusion

This study investigates the importance of WM on human head modeling. In this paper, we implement four- and five-layered head models excluding and including WM compartment. The preliminary results obtained in this research using statistical error quantifications are testified to investigate the effects of excluding and including WM on EEG. Performing different experiments, we find that the head model excluding WM produces 72% and 0.58 average RDM and MAG errors, respectively, whereas the WM inclusion head model produces 9% and 0.36 average RDM and MAG errors, respectively, with their corresponding reference model. Consequently, the EEG model that excludes WM layer causes more dipole eccentricity errors than the EEG model that includes WM layer. This study suggests that an accurate head model requires WM layer to measure error pruned EEG.

Acknowledgement

This project is supported by Australian Research Council Discovery Program DP0665216.

References

[1] Hallez, H., *et al.*, “Dipole estimation errorsdue to differences in modeling anisotropic conductivities in realistic head models for EEG source analysis,” Journal of Phys. Med. and Bio., vol. 53, pp. 1877-1894, 2008.

[2] J. O. Ollikainen, *et al.* “Effects of local skull inhomogeneities on EEG source estimation,” Med. Eng. and Phy., vol. 21, pp. 143-154, 1999.

[3] J. Haueisen, “The influence of forward model conductivities on EEG/MEG source reconstruction,” IEEE Proceedings of NFSI & ICFBI, pp. 18-19, 2007.

[4] P. Wen, “Human Head Modelling and Computation for the EEG Forward Problem,” PhD dissertation, The Flinders University of Western Australia, Australia, 2000.

[5] C. H. Wolters, “Influence of Tissue Conductivity Inhomogeneity and Anisotropy on EEG/MEG based Source Localization in the Human Brain*,”* PhD dissertation, University of Leipzig, France, 2003.

[6] Z. Zhang and D. L. Jewett, “ Insidious error in dipole localization parameters at a single time-point due to model misspecification of number of shells,” Electroence.. Clin. Neurophy.l. vol. 88, pp. 1-11, 1993.

[7] K. Wendel, *et al.*, “The Influence of CSF on EEG Sensitivity Distributions of Multilayered Head Models,” IEEE Trans. on Bio. Engr., vol. 55, no. 4, pp. 1454-1456, 2008.

[8] H. Hallez, *et al.*, “Dipole Localization Errors due to not Incorporating Compartments with Anisotropic Conductivities: Simulation Study in a Spherical Head Model,” IJEM, vol 7, no. 1, pp. 134-137, 2005.

[9] H. Li, *et al.*, “Brain Tissue Segmentation based on DWI/DTI Data,” 3rd IEEE International Symposium on Biomedical Imaging: Nano to Macro, 2006.

[10] S. Kim *et al.*, “Influence of Conductivity Tensors in the Finite Element Model of the Head on the Forward Solution of EEG,” IEEE conference on Nuclear Science Symposium Conference Record, 2001.

[11] L. Li, *et al.,* “A Study of White Matter Anisotropic conductivity on EEG Forward Solutions,” IEEE Proceedings of NFSI & ICFBI, pp.130-132, 2007.

[12] R. Bashar, *et al.*, “Influence of white matter inhomogeneous anisotropy on EEG forward computing,” Australasian Physical & Engineering Sciences in Medicine, vol. 31, no. 2, pp. 122-129, 2008.

[13] R. Bashar, *et al.*, “Tissue Conductivity Anisotropy Inhomogeneity Study in EEG Head Modelling,” Int. Conf. on BioComputing (BioComp’08), USA, 2008.

[14] Mathwork software, The Matlab.

[15] S. Baillet, *et al.*, “Electromagnetic Brain Imaging using Brainstorm,” IEEE Int. Symposium on Bio. Engr.: Macro to Nano, pp. 652-655, 2004.

[16] P. N. Sen and P. J. Basser, “A Model for Diffusion in White Matter in Brain,” Biophysical Journal, vol. 89, pp. 2927-2938, 2005.

[17] T. Liu, *et al.*, “76-space Analysis of Grey Matter Diffusivity: Methods and Application*,*” MICCAI, Palm Springs, California, USA, 2005.